Synthesis and Characterization of Nanostructured Titania Films for Dye-Sensitized Solar Cells

Kyung-Jun Hwang, Seung-Joon Yoo,† Sung-Hoon Jung, Dong-Won Park,‡ Sun-Il Kim, and Jae-Wook Lee*

Department of Chemical and Biochemical Engineering, Chosun University, Gwangju 501-759, Korea
**E-mail: jwlee@chosun.ac.kr*
†Department of Environmental and Chemical Engineering, Seonam University, Namwon 590-711, Korea
‡Advanced Radiation Technology Institute, Korea Atomic Energy Research Institute, Jeongeup, Jeonbuk 580-185, Korea
Received September 10, 2008, Accepted November 24, 2008

The nature and morphology of titanium dioxide films play a significant role in determining the overall efficiency of dye-sensitized solar cell (DSSCs). In this work, the preparation of nanostructured titania particles by sol-gel method (SG-TiO_2) and its characterization were investigated for the application of DSSCs. The samples were characterized by XRD, XPS, FE-SEM, BET and FT-IR analysis. The energy conversion efficiency of SG-TiO_2 was approximately 8.3 % under illumination with AM 1.5 (100 mW/cm^2) simulated sunlight. DSSCs made of SG-TiO_2 nanocrystalline films as photoanodes achieved better energy conversion efficiency compared to those prepared using commercially available Degussa P25.

Key Words: Nanostructured titania films, N719 dye, Dye-sensitized solar cell, Adsorption

Introduction

Silicon-type solar cells have been extensively studied because of their high performance and good stability.[1-2] Compared to the conventional silicon-type cells, dye sensitized solar cells (DSSCs) have been widely investigated because they offer attractive advantages including low cost, less toxic manufacturing, easy scale-up, light weight, and use of flexible panels compared to conventional p-n junction devices.[3-5] Among many metal oxides, nanocrystalline titania materials have been extensively studied because of their interesting physical and chemical properties.

DSSC consists of sensitizing dye, TiO_2 porous film (anode electrode), electrolyte, and opposite electrode (cathode electrode). A light is absorbed by a dye molecule leading to the excitation of the dye to an electronically excited state ($S^*_{adsorbed}$). The excited dye molecule injects an electron into the conducting band of the TiO_2 electrode and is oxidized ($S^+_{adsorbed}$). The original state of the dye ($S_{adsorbed}$) is subsequently restored by electron donation from the electrolyte, usually an organic solvent containing redox system, such as the iodide/triiodide couple. The regeneration of the dye by iodide intercepts the recapture of the conduction band electrons by the oxidized dye. The iodide is in turn regenerated by the reduction of triiodide at the cathode electrode. The circuit is competed by electron migration through an external load.[6,7] It has been known that the nature and morphology of TiO_2 films highly affect the overall conversion efficiency of DSSCs.

This study focused on the synthesis and characterization of nanostructured TiO_2 films for DSSCs. A colloidal SG-TiO_2 suspension was prepared by the sol-gel method based on the hydrolysis of titanium-tetraisopropoxide. The samples were characterized by XRD, XPS, FE-SEM, BET and FT-IR analysis. The solar cell performances of the TiO_2/dye sensitized nanocrystalline solar cells were evaluated from the overall conversion efficiency (η_{eff}), fill factor (*FF*), open-circuit voltage (V_{oc}) and short-circuit current (I_{sc}).

Experimental

A colloidal TiO_2 suspension was prepared by the hydrolysis of titanium-tetraisopropoxide (TTIP, Junsei Chemical Co., > 98%) represented by the following reaction:

$$TTIP + 2H_2O \rightarrow TiO_2 + 4C_3H_7OH \quad (1)$$

TTIP was used as a main starting material without further purification. An appreciated amount (20 ml) of TTIP was slowly dropped in ethanol (200 ml) at room temperature for 5 min. Consequently, a drop-wise addition of hydrochloric acid solution (0.05 M) into the TTIP solution was conducted for 24 h under vigorous stirring condition. The suspension was then ultrasonicated at room temperature for 1 h and centrifugated at -4°C and 8,000 rpm for 20 min. The white precipitate formed was filtered and dried at room temperature for 1 h. Finally, the dried TiO_2 particles were calcined at 450°C for 30 min in air gas flow (5 ml/min). For the preparation of TiO_2 thin-film, TiO_2 slurry was prepared by the addition of 2 g TiO_2 particles, 0.68 ml 10% acetyl acetone, 1 g hydroxypropyl cellulose (Mw. 80,000, Aldrich), and 10.68 ml water for 12 h at 300 rpm using a Zr ball mill (Planetary Mono Mill, FRITSCH). Thus, a TiO_2 film was fabricated by coating a precursor paste onto the fluorine-doped SnO_2 conducting glass plates (FTO, 10 Ω/cm^2, Asahi glass Co., Japan) by using a squeeze printing technique (adhesive tape was used as spacer of ca. 43 μm thickness). The TiO_2 film was treated by heating at 500°C for 2 h because hydroxypropyl cellulose is perfectly removed at over 500°C based on the TG analysis. To fabricate the DSSCs, the prepared thin film electrode was immersed in the N719 dye (Solaronix) solution of 5×10^{-4} M at 80°C for 24 h, rinsed with

anhydrous ethanol and dried. Pt coated glass-SnO_2:F electrode was prepared as a counter electrode. The Pt electrode was placed over the dye-adsorbed TiO_2 electrode, and the edges of the cell were sealed with sealing sheet (SX 1170-60, Solaronix). Sealing was accomplished by hot-pressing the two electrodes together at 80°C. The redox electrolyte was into the cell through the small holes and sealed with a small square of sealing sheet. The redox electrolyte consists of 0.3 M 1,2-dimethyl-3-propylimidazolium iodide (Solaronix), 0.5 M LiI (Aldrich), 0.05 M I_2 (Aldrich), and 0.5 M 4-*tert*-butylpyridine (4-TBP, Aldrich) and 3-metoxypropionitrile as a solvent.

The crystallinity and surface state of the synthesized TiO_2 was characterized by X-ray diffractometer (XRD; D/MAX-1200, Rigaku) using a *CuKα* X-ray and Ni filter at 35 kV and 15 mA. XPS analysis was conducted using a photoelectron spectrometer VG Scientific MultiLab 2000 system equipped with a non-monochromatic *MgKα* radiation of 1253.6 eV. The C1s peak (285.0 eV) was used to calibrate the binding energy values. The film thickness and surface morphology were measured by field-emission scanning electron microscopy (FE-SEM; S-4700, Hitachi). The morphology of the TiO_2 electrode was also examined on an atomic force microscope (AFM; CP-2, VEECO) in the non-contact model. Nitrogen adsorption and desorption isotherms were measured for the BET surface areas, pore size and pore volume at 77 K using a Micromeritics ASAP 2010 automatic analyzer. Before the measurements, the samples were outgassed for 2 h in the degas port of the adsorption apparatus. In addition, the pore size distributions were also calculated from the adsorption branches of the isotherms by using the Barrett, Joyner, and Halenda (BJH) method.[8] Moreover, the Fourier transform infrared spectrophotometer (FT-IR; DA-8, BOMEM) was used for the analysis of the bonding structure between dye molecules and TiO_2 surface. The adsorption amount of TiO_2 film was measured by completely desorbing the adsorbed dye molecules from TiO_2 film using 0.1 M NaOH solution /ethanol (50/50, v/v). The photocurrent-voltage (*I-V*) curves were measured using a source measure unit under irradiation of white light from a 1,000 W Xenon lamp (Thermo Oriel Instruments, USA). The incident light intensity and the active cell area were 100 mW/cm^2 and 0.25 cm^2, respectively. The *I-V* curves were used to calculate the short-circuit current (I_{sc}), open-circuit voltage (V_{oc}), fill factor (*FF*), and overall conversion efficiency (η_{eff}) of DSSCs.

Results and Discussion

The results of the characterization of the SG-TiO_2 nanoparticles are depicted in Figure 1 and Figure 2. Figure 1 shows RD patterns of SG-TiO_2 synthesized in this work and commercial TiO_2 (Degussa P25) with heat treatment at 450 °C for 30 min. SG-TiO_2 showed single-phase anatase nanocrytallites almost without rutile, while P25-TiO_2 has the mixture of anatase and rutile phases (8:2). From the line width of XRD peak of the samples, we have also roughly estimated the particle sizes of TiO_2 using the Scherrer's equation:[9] 22 nm for P25-TiO_2 and 14 nm for SG-TiO_2. XPS analysis provides important information about physicochemical changes of porous materials.

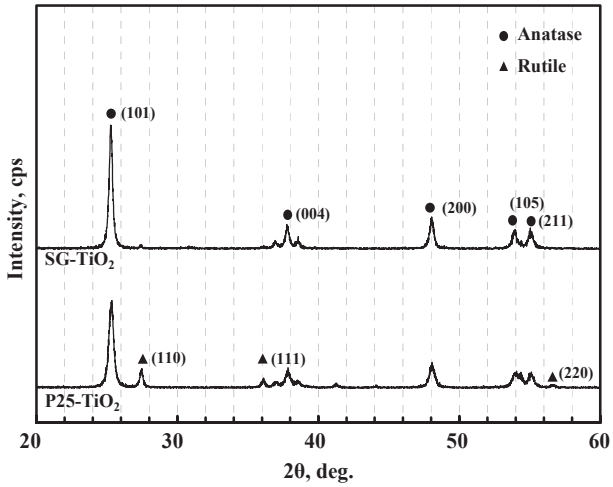

Figure 1. X-ray diffraction spectra of SG-TiO_2 and P25-TiO_2.

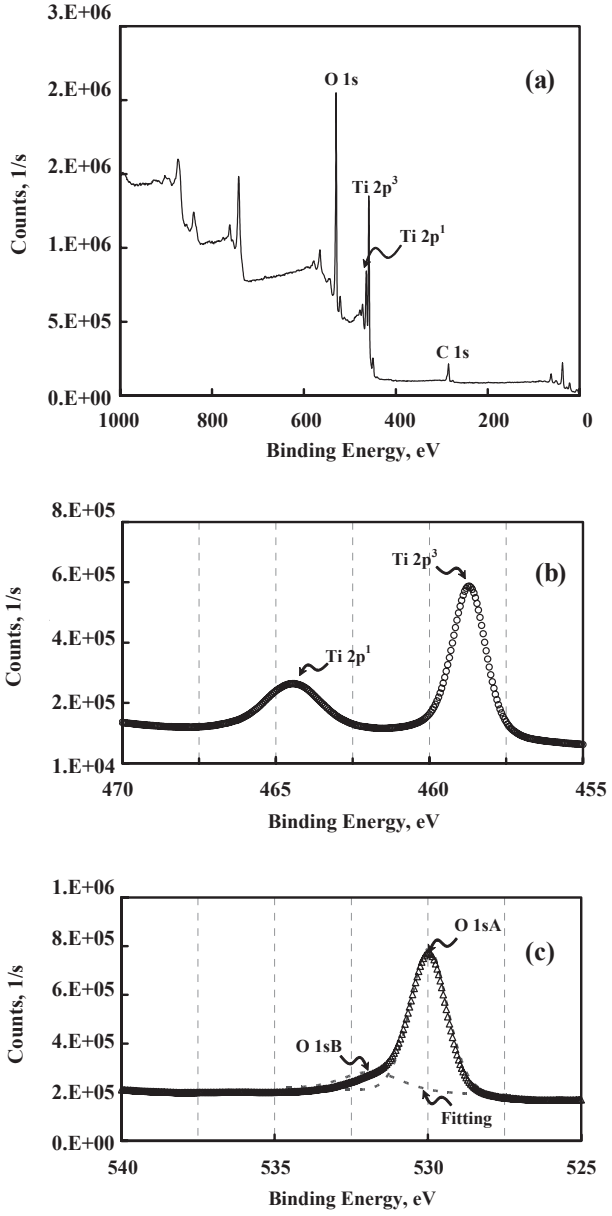

Figure 2. XPS survey spectra of (a) SG-TiO_2 film, (b) Ti 2p core level, and (c) O 1s core level.el, and (c) O 1s core level.

Figure 2 is the quantitative XPS analysis of SG-TiO_2. The survey spectrum of the SG-TiO_2 contains the Ti 2p and O 1s peaks of the titanium dioxide. The Ti $2p^1$ and Ti $2p^3$ spin-orbital splitting photoelectrons are located at binding energies of 464.4 eV and 458.7 eV, respectively (Figure 2(b)). The O 1sA peak of SG-TiO_2 is shown at 530.64 eV and a shoulder located toward the side of higher binding energies (Figure 2(c)). The contents of Ti and O of SG-TiO_2 are 27.01% and 52.23% corresponding to closely Ti^{4+} state. Generally, similar results are observed in TiO_2 porous materials.[10,11]

To characterize the nanocrystalline TiO_2 film properties, FE-SEM, XPS, and BET measurements were performed. Figure 3(a, b) exhibits the FE-SEM images of surface morphology and the cross-section of TiO_2 thin films coated on FTO glass. TiO_2 film has a porous structure in which the TiO_2 spherical nanoparticles are all bonded together through a sintering process. The spherical nanoparticles of P25-TiO_2 (Figure 3(a)) and SG-TiO_2 (Figure 3(b)) are well distributed and maintain their original size and shape. The pattern reveals the TiO_2 particles to be composed of a three-dimensional network of interconnected particles. We also found that the particle size of SG-TiO_2 was smaller than that of P25-TiO_2. The film thickness was ca. 3~4 μm. These results are consistent with those estimated from XRD data. According to the AFM images of P25-TiO_2 (Figure 3(c)) and SG-TiO_2 (Figure 3(d)), the films have heterogeneous surface with a few separated islands. The surface roughness is summarized in Table 1. Thus, it was found from these results that nanoparticle TiO_2 with a well ordered structure and high surface area can be successfully synthesized.

The N_2 adsorption-desorption isotherm and pore size distribution of the samples are depicted in figure 4(a). It was also observed from N_2 adsorpion-desorption isotherm measurement. The physico-chemical properties of commercial P25-TiO_2 and synthesized SG-TiO_2 are listed in Table 2. It has been known that the anatase TiO_2–based solar cells exhibit better photovoltaic characteristics compared to the rutile TiO_2–based solar cells because of higher surface area (i.e., higher amount of dye adsorbed).[12] The surface area determined by nitrogen adsorption/desorption isotherm data of SG-TiO_2 was found to be 69

Table 1. Physico-chemical properties of TiO_2 films

Characteristic	Unit	Degussa P25	SG-TiO_2
Rms Roughness of AFM	Nm	25.14	28.86
Average Roughness of AFM	Nm	20.31	22.96
Adsorption amount of N719	mM/cm^2	7.612×10^{-5}	12.693×10^{-5}

Table 2. Physical properties of TiO_2 particles

Property	Unit	Degussa P25	SG-TiO_2
Surface area (BET)	m^2/g	50[a] (40.19[b])	69.54
Pore volume	cm^3/g	0.19[b]	0.14
Average pore size (BJH)	Å	69[b]	62
Average particle size	nm	approx. 21[a,*]	approx. 15
Density	g/l	approx. 130[a]	128
Purity	%	> 99.5[a]	-

[a]from the manufacturer's report, [b]measured in this work, [*]the size of the primary particles

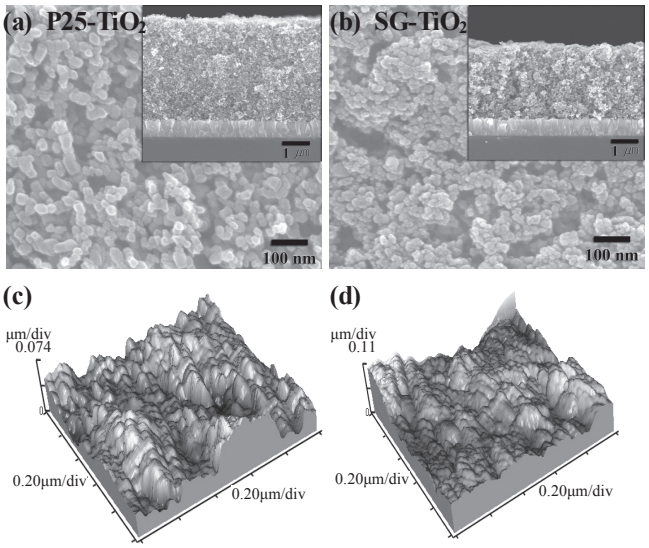

Figure 3. FE-SEM images of (a) P25-TiO_2 film, (b) SG-TiO_2 film and AFM image of (c) P25-TiO_2 film, (d) SG-TiO_2 film.

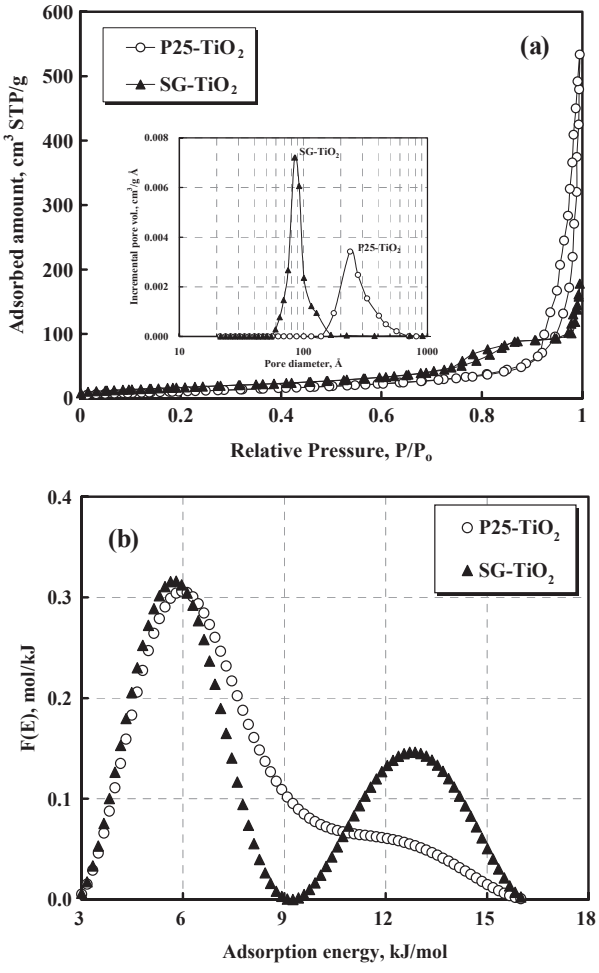

Figure 4. (a) N_2 gas adsorption and desorption isotherms and pore-size distribution of TiO_2 films. (b) Adsorption energy distributions of SG-TiO_2 and P25-TiO_2 films.

m^2/g and the average pore size calculated by BJH method was 62 Å.

Adsorption energy distributions have been extensively applied for characterizing the numerous adsorption systems and understanding the surface energy heterogeneities. In general, geometrical heterogeneity comes from the differences in size and shape of pores while chemical heterogeneity is associated with different functional groups and various surface defects on a surface. The fundamental adsorption integral equation for energetically heterogeneous solid surfaces is given as follows:[13]

$$\theta(p) = \int_{E_{\min}}^{E_{\max}} \theta(p,E) \cdot F(E) \cdot dE \qquad (2)$$

where p is the equilibrium concentration, E is the adsorption energy, $F(E)$ is the adsorption energy distribution function, $\theta(p, E)$ is a local adsorption isotherm with an adsorption energy, $\theta(p)$ is the experimental adsorption isotherm data. The adsorption integral equation is the well-known linear Fredholm integral equation of the first kind, and the calculation of adsorption energy distribution is an ill posed problem.[14] The generalized nonlinear regularization method can avoid the difficulties resulting from the ill-posed nature of an adsorption integral equation.[15] In this work, therefore, we employed the generalized nonlinear regularization method based on smoothness constraint (i.e., Tikhonov regularization) and edge preserving regularization methods.[16]

Figure 4(b) shows the adsorption energy distribution functions of TiO_2 films formed on the FTO glass. The adsorption energy distribution curves of SG-TiO_2 synthesized in this work exhibited two peaks indicating the existence of energetically two different adsorption sites. The first and second adsorption energy curves were distributed mainly in the range of 3~9 and 9~16 kJ mol^{-1}, respectively. The energy intensity of the first peak is about 2 times higher than that of the second one. However, the second peak of P25-TiO_2 was not evident compared to the synthesized SG-TiO_2 samples. The energy distribution peaks proceeded to higher energy with the increase of surface area (Table 2). The increase of surface area (i.e., increase in adsorption capacity of dye molecules) will served for the enhanced energy conversion efficiency of DSSCs. It was also found that the shape and the intensity of the adsorption energy distribution curve were highly related with the physical property (i.e., geometrical heterogeneity) and chemical characteristics (i.e., energetic heterogeneity) of nanocrystalline TiO_2 for DSSCs. The results can be successfully applied for the design, synthesis and optimization of nanocrystalline TiO_2 for DSSCs because the adsorption energy distribution functions obtained in this work will offer the fundamental and informative data to fully understand the surface heterogeneity of the nanostructured TiO_2 materials.

Interfacial binding between the dye molecules (N719) and the surface of TiO_2 was investigated by FT-IR spectra of the dye-anchored TiO_2 films. In general, the efficiency of the charge injection process is highly dependent on bonding structure of the dye molecules adsorbed on the TiO_2 film. In addition, the electron transfer in DSSC is strongly influenced by

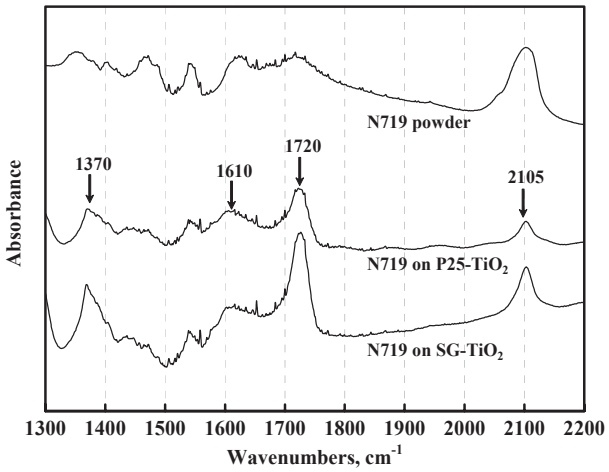

Figure 5. FT-IR spectra of N719 dye adsorbed on TiO_2 films compared to the signals of the N719 dye powder.

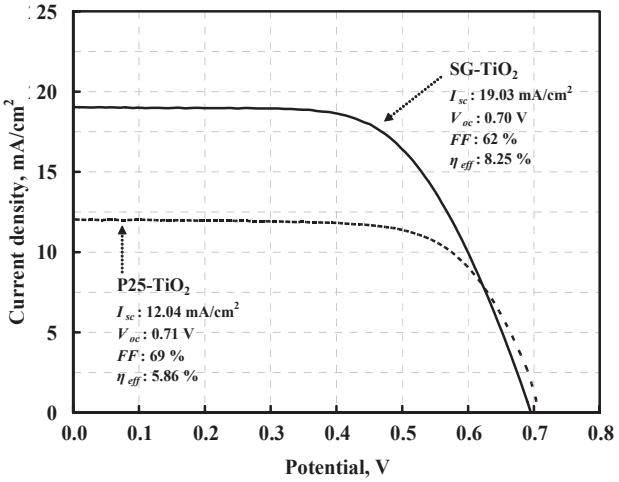

Figure 6. Photocurrent-voltage (I-V) curves of SG-TiO_2 and P25-TiO_2 films.

electrostatic and chemical interactions between TiO_2 surface and the adsorbed dye molecules.[17] Figure 5 shows the FT-IR spectra of N719 dye adsorbed on TiO_2 films (P25-TiO_2, SG-TiO_2) compared to the signals of the dye powder. Absorption at 2105 cm^{-1} of N719 dye is attributed to the SCN stretch model of N-bonded SCN ligand.[18,19] The IR spectra were observed at 1370 cm^{-1}, 1610 cm^{-1}, and 1720 cm^{-1}A when the dye molecules were adsorbed on P25-TiO_2 and SG-TiO_2 films. The IR spectra located at 1370 cm^{-1} and 1610 cm^{-1} is consistent with the bidentate coordination. Compared to the dye-anchored P25-TiO_2 films, the dye-anchored SG-TiO_2 films have strong absorptions at 1720 cm^{-1}, indicating the C=O stretch mode of the protonated carboxylic acid (i.e., ester-like linkage). Similar results were reported that the coordination of N719 dye on TiO_2 films occurs mainly by the contribution of unidentate (i.e., ester-like linkage) and partially by bidentate linkage.[17-19]

Figure 6 shows the photocurrent-voltage curves of P25-TiO_2 and synthesized SG-TiO_2. The fill factor (*FF*) and overall energy efficiency (η_{eff}) were determined by the equations which was described in detail elesewhere.[7,20] A dye-sensitized

solar cell assembled with SG-TiO_2 gave an open-circuit voltage of 0.70 V and short-circuits current density of 19.03 mA/cm^2 for an incident light intensity of 100 mW/cm^2. The power conversion efficiency of over 8.3 % was achieved using the single-phase anatase crystallites synthesized (SG-TiO_2) in this work. It was found that DSSCs made of nanostructured SG-TiO_2 films showed better photoelectrochemical properties compared to those prepared using Degussa P25-TiO_2 films.

Conclusions

The colloidal TiO_2 suspension was prepared by sol-gel method based on the hydrolysis of titanium-tetraisopropoxide. The TiO_2 films of single-phase anatase crystallites were formed on the FTO glass for a working electrode of DSSCs. The films were characterized by XRD, XPS, FE-SEM, AFM, and BET anaysis. The contents of Ti and O of SG-TiO_2 are 27.01 % and 52.23 % corresponding to closely Ti^{4+} state. The nanoparticle size of SG-TiO_2 is about 14 nm and the film thickness was *ca.* 3~4 μm. According to the AFM image, the films have heterogeneous surface with a few separated islands. A dye-sensitized solar cell of SG-TiO_2 gave an open-circuit voltage of 0.70 V and short-circuits current density of 19.03 mA/cm^2 for an incident light intensity of 100 mW/cm^2. It was found that DSSCs made of SG-TiO_2 nanocrystalline films as photo-anodes achieved better photo-energy conversion efficiency compared to those prepared using commercially available Degussa P25 films. The power conversion efficiency of over 8.3% was achieved using the single-phase anatase SG-TiO_2 crystallites synthesized in this work.

Acknowledgments. This work was supported by the Korea Research Foundation Grant funded by the Korean Government (MOEHRD) (KRF-2007-H00023). Also, this research was financially supported by the Ministry of Education, Science Technology (MEST) and Korea Industrial Technology Foundation (KOTEF) through the Human Resource Training Project for Regional Innovation.

References

1. O'Regan, B.; Grätzel, M. *Nature* **1991**, *353*, 737.
2. Kazmerski, L. L. *J. of Electron Spectroscopy and Related Phenomena* **2006**, *150*, 105.
3. Ko, Y. S.; Kim, M. H.; Kwon, Y. U. *Bull. Korean Chem. Soc*. **2008**, *29*(2), 463.
4. Kang, M. G.; Ryu, K. S.; Chang, S. H.; Park, N. G.; Hong, J. S.; Kim, K. J. *Bull. Korean Chem. Soc*. **2004**, *25*(5), 742.
5. Hoshikawa, T.; Ikebe, T.; Yamada, M.; Kikuchi, R.; Eguchi, K. *J. Photochem. Photobiol. A* **2006**, *184*, 78.
6. Xia, J.; Li, F.; Huang, C.; Zhai, J.; Jiang, L. *Solar Energy Materials & Solar Cells* **2006**, *90*, 944.
7. Kalyanasundaran, K.; Grätzel, M. *Coordination Chemistry Reviews* **1998**, *177*, 347.
8. Barrett, E. P.; Joyner, L. G.; Halenda, P. P. *J. Am. Chem. Soc*. **1951**, *73*, 373.
9. Scherrer, P. *Math. Phys.* **1918**, *2*, 98.
10. Gratzel, M. *Prog. Photovolt. Res. Appl*. **2000**, *8*, 171.
11. Moudler, J. F.; Stickle, W. F.; Sobol, P. E.; Bomben, K. D. *Handbook of X-ray Photoelectron Spectroscopy*; Eden Praitie Perkin-Elmer: MN, 1992.
12. Park, N. G.; Frank, A. J. *J. Phys. Chem. B* **2000**, *104*(38), 8989.
13. Puziy, A. M.; Matynia, T.; Gawdzik, B.; Poddubnaya, O. I. *Langmuir* **1999**, *15*, 6016.
14. Szombathely, M. V.; Brauer, P.; Jaroniecl, M. J. *Comput. Chem.* **1992**, *13*, 17.
15. Roth, T. M.; Weese, J.; Honerkamp, J. *Comput. Phys. Commun.* **2001**, *139*, 279.
16. Weese, J. *Comput. Phys. Commun.* **1992**, *69*, 99.
17. Hwang, K. J.; Yoo, S. J.; Kim, S. S.; Kim, J. M.; Shim, W. G.; Kim, S. I.; Lee, J. W. *J. Nanosci. Nanotechnol.* **2008**, *8*, 4976.
18. Leon, C. P.; Kador, L.; Peng, B.; Thelakkat, M. *J. Phys. Chem. B* **2006**, *110*(17), 8723.
19. Finnie, K. S.; Bartlett, J. R.; Woolfrey, J. L. *Langmuir* **1998**, *14*, 2744.
20. Grätzel, M. *J. Photochem. Photobiol. C* **2003**, *4*, 145.